PCCP

Accepted Manuscript

This is an *Accepted Manuscript*, which has been through the Royal Society of Chemistry peer review process and has been accepted for publication.

Accepted Manuscripts are published online shortly after acceptance, before technical editing, formatting and proof reading. Using this free service, authors can make their results available to the community, in citable form, before we publish the edited article. We will replace this *Accepted Manuscript* with the edited and formatted *Advance Article* as soon as it is available.

You can find more information about *Accepted Manuscripts* in the Information for Authors.

Please note that technical editing may introduce minor changes to the text and/or graphics, which may alter content. The journal's standard Terms & Conditions and the Ethical guidelines still apply. In no event shall the Royal Society of Chemistry be held responsible for any errors or omissions in this *Accepted Manuscript* or any consequences arising from the use of any information it contains.

ROYAL SOCIETY OF CHEMISTRY

www.rsc.org/pccp

The Interactions between TiO_2 and Graphene with Surface Inhomogeneity determined using Density Functional Theory

Brandon Bukowski, N. Aaron Deskins*

Worcester Polytechnic Institute

Department of Chemical Engineering

Worcester, MA 01609

* Corresponding author: nadeskins@wpi.edu

Abstract:

TiO_2/graphene composites have shown promise as photocatalysts, leading to improved electronic properties. We have modeled using density functional theory TiO_2/graphene interfaces formed between graphene with various defects/functional groups (C vacancy, epoxide, and hydroxyl) and TiO_2 clusters of various sizes. We considered clusters from 3 to 45 atoms, the latter a nanoparticle of ~1 nm in size. Our results show that binding to pristine graphene is dominated by van der Waals forces, and that C vacancies or epoxide groups lead to much stronger binding between the graphene and TiO_2. Such sites may serve to anchor TiO_2 to graphene. Graphene surfaces with hydroxyls however lead to OH transfer to TiO_2 and weak interactions between the graphene and the hydroxylated TiO_2 cluster. Charge transfer may occur between TiO_2 and graphene in various directions (graphene to TiO_2 or TiO_2 to graphene), depending on the state of the graphene surface, based on overlap of the density of states. Our work indicates that graphene surface defects or functional groups may have a significant effect on the stability, structure, and photoactivity of these materials.

Physical Chemistry Chemical Physics Accepted Manuscript

1. Introduction

Graphene has received enormous attention since its discovery and has been pursued for catalytic, photocatalytic, energy storage, electronic, and various other purposes[1-7]. It has unique electronic properties (e.g. high electron mobility) and is composed of an abundant element, namely carbon, which makes it economically attractive. Graphene/semiconductor composites show promise for use in photocatalytic, photovoltaic, and electrochemical devices[1, 8-10]. One such promising composite is graphene/TiO_2. TiO_2 is a prototypical metal oxide used for photocatalytic and photovoltaic processes. In such composites a number of interesting effects are proposed to occur during photocatalysis[1]. The semiconductor (such as a metal oxide) may enable photoexcitation of electrons, while the graphene may act as a fast charge transporter. Such materials may impair electron-hole recombination (such recombination limits the net photoexcitation yield) by exploiting the higher mobility of charge transferred into the graphene sheet and thus separating holes and electrons generated in the semiconductor. The presence of graphene may also act as a sensitizer by extending photo-absorption into the visible region[11-13]. Finally new reaction sites may exist at the interface, which increase the overall reactivity. Identifying the reasons as to why graphene-based composite materials behave so well and strategies for improving such composites is an important, on-going area of research.

A number of experimental studies have been performed on graphene/TiO_2, as attested by recent review articles[1, 9, 14, 15]. There have also been several theoretical studies of graphene/TiO_2 materials using density functional theory (DFT). Some papers have focused on smaller TiO_2 clusters (a prototype for larger TiO_2 materials), typically 3 to 12

Physical Chemistry Chemical Physics Accepted Manuscript

atoms in size[16-22]. Both pure graphene, as well as graphene with functional groups/defects have been considered in these small cluster studies. Binding energies of the TiO_2 clusters to graphene and their electronic configurations (e.g. density of states) have typically been calculated in these studies. New electronic states can form as the graphene and TiO_2 interact with each other, which can potentially improve photocatalytic properties of the graphene/TiO_2 system[16]. It was also found that strong interactions between adsorbed molecules, such as H_2 or CO, occur with the composite materials[19-21]. A recent paper modeled Fe-doped TiO_2 nanostructures (up to 48 atoms) over graphene and found strong binding between the graphene and TiO_2 at graphene carboxylate sites[23].

Still another set of other papers has modeled extended TiO_2 surfaces interacting with pristine (meaning defect-free herein) graphene sheets[13, 24-29]. These studies have employed periodic boundary conditions to model surfaces of TiO_2 (either anatase or rutile phases) and have provided many details on the electronic structure of such graphene composites. These previous DFT results show that new electronic bands (compared to TiO_2 or graphene alone) may occur in TiO_2/graphene composites, and these states may explain the increased photo-activity of TiO_2/graphene composites. Charge separation (which leads to more photoexcitation yield) may occur due to physically separated electronic bands on the two materials[13, 24, 27]. The band gap of composite may also be reduced, leading to potential photoabsorption in the visible region of light[25, 27, 30]. Another paper[31] modeled graphene/glycine/TiO_2 systems, and also modeled graphene oxide in the vicinity of glycine or TiO_2. Thin-layer anatase over graphene and graphene oxide have also been simulated[32]. These DFT papers have provided much insight on graphene/TiO_2 systems, but full details on the effect of graphene defects or surface functional groups in

Physical Chemistry Chemical Physics Accepted Manuscript

these composites are still unknown. Several papers even present contradictory results (such as in photoexcitation analysis)[25, 27, 32], further confusing our understanding of these materials.

Indeed, defects and surface groups may be very prevalent in many graphene systems. There are several methods to synthesize graphene, involving chemical, physical, and mechanical approaches[33-35]. The properties of graphene sheets may vary depending on the type and quantity of defects and surface groups[36, 37]. A common approach[38] forms graphene oxide (which consists of graphene with various chemical groups such as hydroxyls, carboxyls, or epoxides) from pure graphite. Exfoliated or separated graphene oxide sheets are further reduced to form reduced graphene oxide (rGO). The aim of producing rGO is to obtain sheets as close as possible to pristine graphene. rGO however may have a significant number of defects and surface species. Previous literature results also indicate that the O content may be significant in reduced graphene oxide[38-40]. Graphene oxide/TiO_2 composites have also been shown to be promising photocatalysts[41, 42].

The current paper was motivated to understand many of the details of the interface between TiO_2 and non-pristine graphene (i.e. containing defects or oxygen-containing groups). Several of the TiO_2 cluster/graphene studies[16-21] considered graphene with vacancies, hydroxyls, or oxygen-containing groups, but only modeled small TiO_2 molecular species. The work on TiO_2 slabs/graphene systems has tended to only consider pure graphene. The current paper provides more details on TiO_2/graphene composites by using DFT to model TiO_2 clusters in various sizes (up to ~1 nm in size or 45 atoms) and graphene. Interactions between large TiO_2 clusters and graphene have not been

Physical Chemistry Chemical Physics Accepted Manuscript

previously performed. We consider in this work pure graphene, as well as graphene sheets with hydroxyl groups, epoxy groups, and C vacancies. We modeled several TiO_2 clusters over graphene. Our work highlights the important role that graphene defects and surface groups may play in graphene/TiO_2 systems.

2. Computational Methodology

We performed spin-polarized DFT calculations with the mixed Gaussian and plane wave (GPW) approach[43] to optimize the graphene/TiO_2 structures. A double zeta basis set[44] was used for all atom types to treat valence electrons, while pseudopotentials of the Goedecker-Teter-Hutter type[45, 46] were used for core electrons. The exchange-correlation functional used was the Perdew, Burke, Ernzerhoff (PBE) functional[47]. Van der Waals forces were approximated using the correction of Grimme[48]. All geometry relaxations were performed with the CP2K code[49, 50], utilizing periodic boundary conditions. Only the gamma point was sampled in reciprocal space. Calculations were spin-polarized.

Once optimized geometries were found using the CP2K code, single point calculations using the Vienna *ab initio* software package (VASP)[51-54] were performed to obtain accurate electronic structures and density of states (DOS). The VASP calculations used a 4x4x1 *k*-point mesh with a 400 eV energy cutoff for the plane-wave basis set. Core electrons were treated by planewave augmented wavefunction (PAW) potentials[55, 56]. We applied a U correction on the VASP calculations in order to get more accurate electronic states. We used the approach of Dudarev et al.[57] and a U value of 4.5 eV applied to the Ti d states. In our previous work[58] we used a U value of 4.5 eV for plane

Physical Chemistry Chemical Physics Accepted Manuscript

wave calculations, which is similar to the 4.2 eV value utilized by Morgan and Watson[59, 60] and Shibuya et al[61]. A U value of 4.5 eV has also been used by other work[62, 63, 64], particularly since this U value. One paper[65] modeled TiO_2 clusters and indicated that a U value of 4.5 eV was suitable for such work. Our choice of 4.5 eV for the U value is therefore in alignment with previous literature values. Overall, this combination of CP2K and VASP allowed fast, efficient optimization (CP2K) combined with accurate calculations of electronic structure (VASP).

The structures of $(TiO_2)_n$ clusters were taken from the work of Qu and Kroes[66] for n=1, 3, 5, and 8, and from Hamad et al.[67] for the n = 15 cluster. Structures from these reports were re-optimized using CP2K and are shown in Figure 1. This last cluster of n=15 had a diameter near 9 Å, or ~ 1 nm. The adsorption energies of clusters bound to the graphene surfaces were defined as follows:

$$E_{adsorption} = E_{(TiO_2)n+graphene} - (E_{(TiO_2)n} + E_{graphene}) \qquad (1)$$

A graphene (6x6) surface supercell was constructed for the simulations and had dimensions of 14.82 Å x 14.82 Å x 25.00 Å with two non-orthogonal surface vectors. This supercell is shown in Figure 3a. The graphene lattice parameter was determined by minimization of the lattice parameter with respect to energy, and found to be 2.47 Å, in good agreement with the experimental value of 2.46 Å. Various defects were added to the sheet, as discussed further. The large vacuum spacing of 25 Å ensured that graphene sheets did not interact with each other.

As Figure 3 shows, the graphene surface has a honeycomb shape where each carbon atom is bound to three surrounding carbon atoms. There are three high-symmetry adsorption sites, being top over a carbon atom, bridging between two carbon atoms, and

Physical Chemistry Chemical Physics Accepted Manuscript

over a hollow site surrounded by six carbon atoms. The inclusion of defects or surface groups further complicates the adsorption process. Our strategy for adsorption of the TiO_2 clusters was to place the clusters at several initial configurations and allow full geometry optimization. This approach gave several stable adsorption sites for each cluster. We report only the most stable sites in the main body of the text.

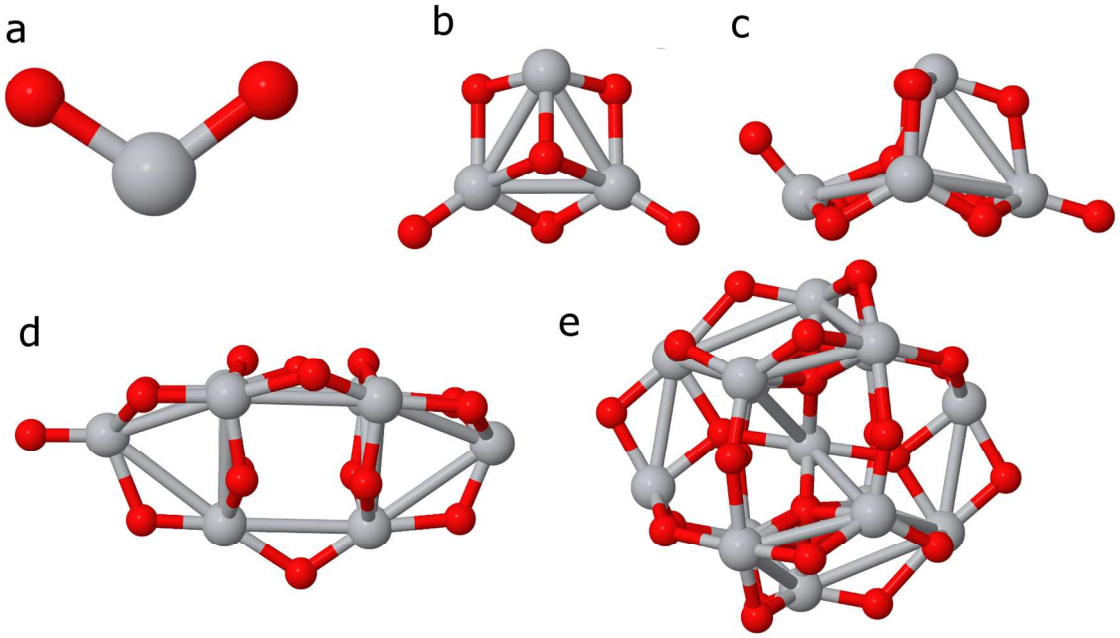

Figure 1. Illustration of $(TiO_2)_n$ clusters modeled in the current work. We considered clusters with n=1,3,5,8, and 15. Ti atoms are represented by grey spheres while O atoms are represented by red spheres.

We performed several tests to determine the accuracy of our method. We adsorbed $(TiO_2)_1$ and $(TiO_2)_3$ clusters over pristine graphene surfaces and compared with literature values. We calculated adsorption energies of -1.15 eV and -1.57 eV for n=1 and n=3 clusters, respectively. For the n = 1 cluster, several adsorption energies in the literature have been reported: -0.8 eV[17], -1.22 eV[18], -1.27 eV[20], and -1.55 eV[19]. Geng et al.[16] calculated an adsorption energy of -1.08 eV for an n=3 cluster. Our current

Physical Chemistry Chemical Physics Accepted Manuscript

computational approach gives adsorption energies in reasonable agreement with previous literature values, which were largely based on calculations using a plane-wave basis set while we used a Gaussian basis set. We also calculated band gaps of the bare lone TiO_2 clusters and compare with literature values in Figure 2. Our band gaps were calculated using the VASP program since VASP provides robust k-point sampling, a necessity for accurate electronic structures. The reference DFT values were taken from various papers in the literature[66, 68, 69]. Two of the papers shown in Figure 2[66, 68] used the B3LYP exchange correlation functional (see References 70, 71 for further details on the B3LYP functional) and Gaussian basis set, which could explain why these two data sets disagree by 1 to 2 eV from our calculated band gaps. Values from Calatayud and Minot[69] were performed using VASP, although with ultrasoft pseudopotentials[72, 73] and a different functional, PW91[74]. Some geometries also differed from our paper and that of Calatayud and Minot, in part due to the difficulty in identifying ground-state structures for such clusters. Our band gap results, however, do show good agreement with these previous DFT calculations and the overall trends with regards to cluster size are consistent across the different calculations. We further note that the current work utilized the PBE functional which is a common generalized gradient approximation (GGA) functional while other previously-mentioned work may have used other functionals, such as B3LYP or PW91. Thus we do not expect the calculated numbers (whether binding energies or band gaps) to agree exactly when comparing our results with all other work. But even when using different functionals the calculated binding energies or band gaps should give similar answers, at least similar order of magnitude or having similar trends. Our analysis

Physical Chemistry Chemical Physics Accepted Manuscript

here indicates that our work is consistent with previous work, giving confidence to our results.

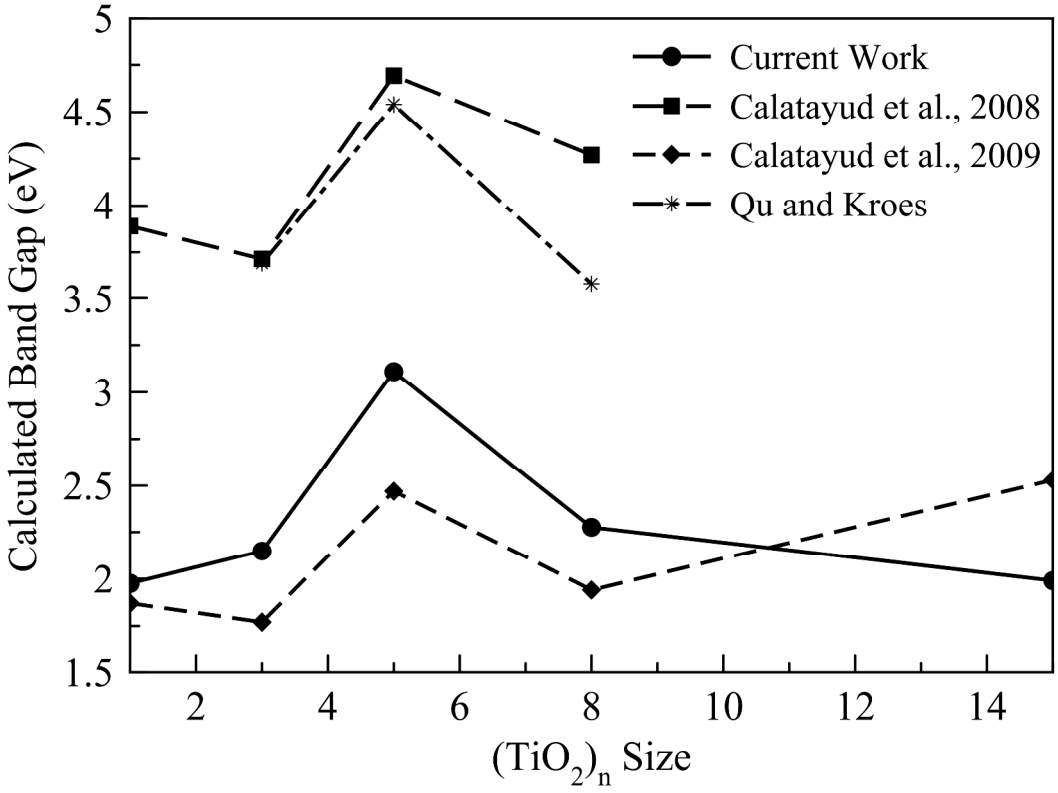

Figure 2. Calculated band gaps of gas-phase clusters from the current work compared to results from the literature[66, 68, 69].

We also briefly discuss the van der Waals correction used in this work. As a matter of practicality we have used the Grimme-type corrections[48] since this method was the van der Waals method implemented in the CP2K version we started this work with. Newer corrections have become available in subsequent versions that specifically include nonlocal additions to the exchange correlation functional to account for dispersion, namely the DF[75] and DF2[76] functionals. We ran select calculations with the n = 1 to 5 clusters over graphene surfaces to test the how these different van der Waals corrections could affect our results. Table 1 gives a summary of these calculations. The results show

Physical Chemistry Chemical Physics Accepted Manuscript

that the Grimme-type corrections overbind the clusters in all cases compared to the nonlocal functional methods but that the differences however are typically on the order of 0.2-0.3 eV, a relatively small difference. There are a variety of other functionals that account for dispersion and it is unclear which approach should be used in the current system. The trends in adsorption and overall conclusions however are not affected by the use of the Grimme-type corrections, and we therefore used this method in the current work.

Table 1. Adsorption energies in eV for the n = 1 to 5 TiO_2 clusters over pristine graphene surfaces with various van der Waals corrections.

	TiO_2 Cluster		
van der Waals Correction Method	n = 1	n = 3	n=5
No Correction	-0.77	-0.98	-0.36
DFT-D2*	-1.15	-1.57	-1.24
vdW-DF	-0.78	-1.21	-0.94
vdW-DF2	-0.92	-1.31	-0.94

* Used in the current work.

3. Results and Discussion

3.1 TiO_2 Clusters

We first optimized lone $(TiO_2)_n$ clusters as presented in Figure 1. We modeled clusters with n = 1, 3, 5, 8, and 15; or 3, 9, 15, 24, or 45 total atoms respectively for the clusters. For each given cluster size there are a number of possible structural isomers. We only considered the most stable, as identified by the works of Qu and Kroes[66] for $n \leq 8$ and Hamad et al.[67] for n = 15. In bulk TiO_2 Ti atoms bond to six O atoms, and O atoms bond to three Ti atoms. Because of their small size, a number of atoms in the clusters are under-coordinated, especially the surface atoms. Generally under-coordinated atoms tend to be the most reactive.

Physical Chemistry Chemical Physics Accepted Manuscript

The clusters we used in this study can be described as follows. The n=1 cluster had a bent geometry with the Ti atom bond to two O atoms, designated Ti_{2c} to indicate coordination, while the O atoms only bond to one Ti atom, designated O_{1c} or one-coordinated. The n=3 cluster had two Ti_{3c} and one Ti_{2c}, as well as O_{1c}, O_{2c}, and O_{3c}. In the n=5 cluster all Ti atoms were four-coordinated, while there were two O_{1c}, one O_{4c}, and seven O_{2c}. In the n=8 cluster all Ti atoms were four-coordinated, with the exception of one Ti which was three-coordinated. The O atoms were all two-coordinated, except one O atom which was one-coordinated. Finally, in the n=15 cluster there were one Ti_{6c}, eight Ti_{5c}, and six Ti_{4c}. All the O atoms were two-coordinated, except three atoms which were three-coordinated and three others which were four-coordinated. Thus, as cluster sizes increased, the atoms tend to adopt higher coordination, and eventually will adopt bulk coordination with appropriate cluster size.

3.2 Graphene surfaces

We considered four different graphene surfaces in this work: pure graphene, graphene with a hydroxyl defect, epoxide defect, and C vacancy. The surfaces are shown in Figure 3. Epoxide defects were introduced into the supercell by adsorbing single oxygen atoms on the surface and in the relaxed geometry the oxygen atom prefers to occupy a bridge site. Hydroxyl defects on the graphene surface were modeled by adsorbing an OH group at a top site. Such geometries for hydroxyl and epoxide groups have been shown previously (see for example Ref. [77]). We also modeled surfaces with a single C vacancy, a defect experimentally observed that leads to a slight distortion around the vacancy site[36]. The rationale behind using these surfaces was to model how the TiO_2

Physical Chemistry Chemical Physics Accepted Manuscript

would interact with flat graphene sheets as well as defects that are expected to form during typical synthesis procedures.

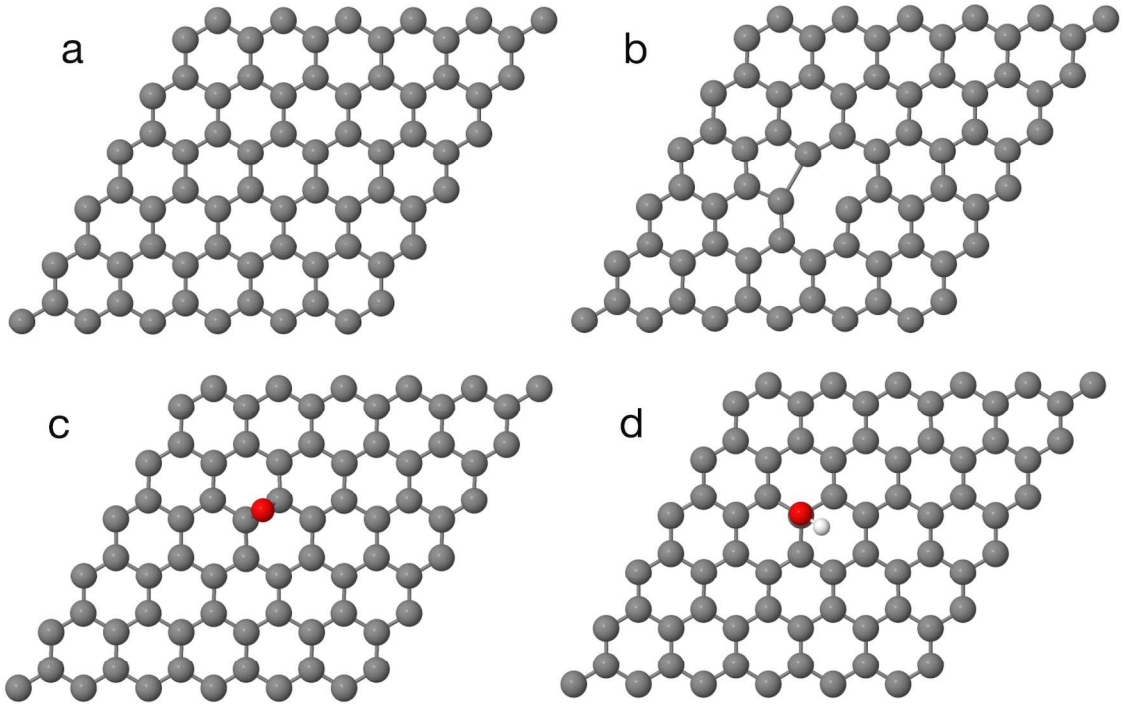

Figure 3. Illustration of graphene surfaces used in the current work. (a) pristine graphene. (b) graphene with C vacancy. (c) graphene with epoxide. (d) graphene with hydroxyl. C atoms are represented by dark grey spheres, O atoms are represented by red spheres, and H atoms are represented by white spheres.

3.3. TiO_2 over pristine graphene

We modeled adsorption of the various TiO_2 clusters over pristine (defect-free) graphene, as shown in Figure 4. These results were obtained utilizing the CP2K program, and notably PBE exchange correlation functional and Grimme-type van der Waals corrections. All the TiO_2 clusters were bound to the surfaces with adsorption energies in

Physical Chemistry Chemical Physics Accepted Manuscript

the range of -1.15 and -1.57 eV (see Table 1), and binding distances (either lowest Ti-C or O-C distances) varied between 2.43 and 2.87 Å. The n = 1 cluster had an adsorption energy of -1.15 eV, and was bound through a Ti-C interaction where the Ti atom was slightly off from the top site. The smallest Ti-C distance was 2.51 Å while the smallest O-C distance was 3.10 Å. There were a number of adsorption geometries (not shown) with similar adsorption energies (within 0.05 eV) indicating poor adsorption site selectivity. Cluster sizes of n=3 and 5 showed similar results with Ti-C distances being 2.43 and 2.67 Å (2.99 and 2.89 Å for O-C distances), while most stable adsorption energies were calculated to be -1.57 and -1.24 eV, respectively. For the n=1,3, and 5 clusters at least one Ti atom (see Figure 4) appears to bind with the graphene surface. We mention previous DFT studies that modeled TiO_2 clusters over pristine graphene. Adsorption energies for the n = 1 cluster have been reported to be -0.8 eV[17], -1.22 eV[18], -1.27 eV[20], and -1.55 eV[19]. These values are similar to calculated adsorption energy of -1.15 eV. For n = 3, values of -1.08 eV[16] and -3.43 eV[22] have been reported. This latter value is inconsistent with the current results (calculated to be -1.57 eV), and this same reference indicated that van der Waals corrections had negligible effect on their adsorption energy, which is also inconsistent with the current results (discussed below). Results for larger clusters (n of 5 or greater) are unavailable in the literature to the author's best knowledge.

Physical Chemistry Chemical Physics Accepted Manuscript

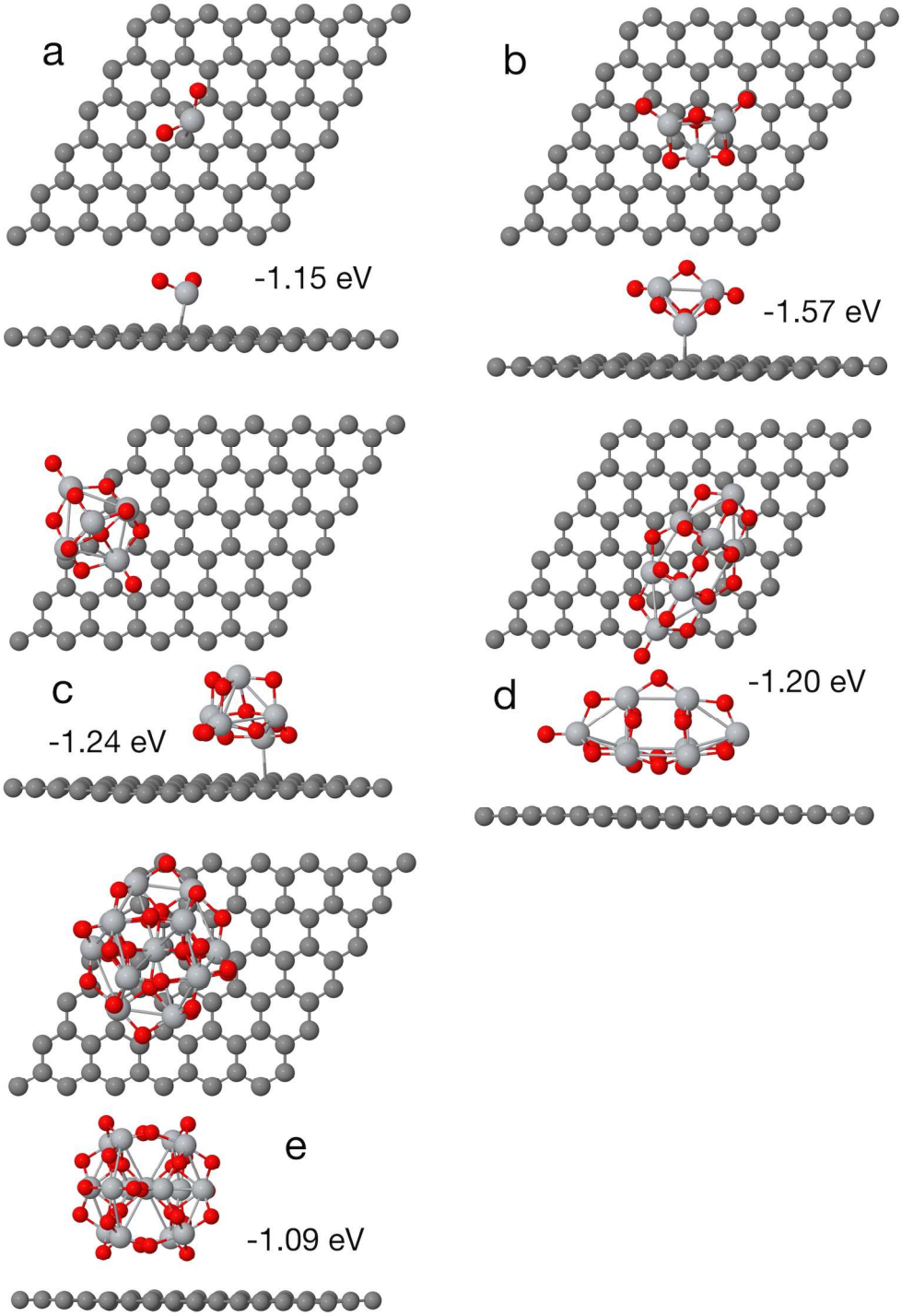

Figure 4. Most stable adsorption sites of TiO_2 clusters over pristine graphene. Results are for clusters of size (a) n=1, (b) n=3, (c) n=5, (d) n=8, and (e) n=15. Color scheme is same as Figures 1 and 3 with light grey spheres representing Ti atoms. The numbers indicate the adsorption energies.

Physical Chemistry Chemical Physics Accepted Manuscript

Table 2. Calculated adsorption energies for the TiO_2 clusters over various graphene surfaces. Values are given in eV. Results were obtained with the CP2K program utilizing the PBE exchange correlation functional and van der Waals corrections of Grimme.

TiO_2 Cluster Size	Pristine Graphene	Graphene with C Vacancy	Graphene with Epoxide	Graphene with Hydroxyl
1	-1.15	-4.60	-2.47	-2.88
3	-1.57	-2.36	-2.93	-3.59
5	-1.24	-1.50	-2.48	-2.40
8	-1.20	-1.75	-2.53	-2.75
15	-1.09	-2.35	-2.93	-3.05

We further explored the adsorption energy landscape for the n = 1 cluster by moving the cluster across the surface, fixing the Ti atom's x- and y-coordinates while allowing the rest of the surface and cluster to relax. In this manner we were able to further quantify how the TiO_2 cluster may interact with a graphene surface. A plot showing adsorption energies with the Ti atom fixed at different locations on the surface can be found in Figure 5. The different adsorption positions of the TiO_2 cluster differ at most by only 0.05 eV. This plot shows that the adsorption energy landscape is very flat, and that the TiO_2 cluster can freely move across the graphene surface and is rather mobile. Similar results were reported by Ayissi et al.[18] The lack of strong distinctive adsorption sites on the surface suggests that strong chemical bonding (e.g. covalent) between TiO_2 and pristine graphene is not occurring.

Physical Chemistry Chemical Physics Accepted Manuscript

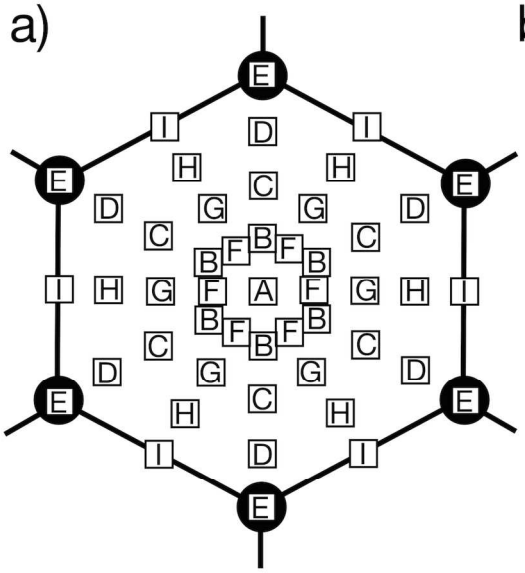

Figure 5. Calculated binding energies of the n=1 TiO_2 cluster to graphene at various locations on a pristine graphene surface. (a) Indication of sites where the cluster was adsorbed. Site A is at the hexagonal site (in middle of graphene hexagon) while site E is on top of a C atom. (b) Calculated adsorption energies corresponding to the different sites.

Indeed, the bonding mechanism between the pristine graphene and TiO_2 appears to primarily involve van der Waals forces. We confirmed this by running adsorption calculations without van der Waals forces. Our original calculations included van der Waals corrections[48], and when we re-ran the calculations without these corrections the adsorption energies declined significantly, as shown in Figure 6. The adsorption energies without the van der Waals corrections varied between -0.98 (n=3) and -0.29 (n=8) eV. The small clusters had adsorption energies of -0.77 eV (n=1) and -0.98 eV (n=3). The larger clusters had much smaller adsorption energies of -0.36 eV (n=5), -0.29 eV (n=8), and -0.37 eV (n=15). The larger clusters were less bound to the graphene surface by ~1 eV without van der Waals corrections. Smaller clusters have more under-coordinated surface atoms, and therefore are more reactive than larger clusters, which explains why

Physical Chemistry Chemical Physics Accepted Manuscript

strong adsorption energies are observed for the small clusters even without van der Waals corrections but not for the large clusters. Because it is defect-free, the pristine surface does not provide adsorption sites for strong binding of TiO_2 since the C atoms of graphene essentially have filled sp^2 orbitals. In summary, our calculations show that over pristine graphene van der Waals forces are the dominant mechanism of adhesion for TiO_2, and that strong covalent bonding is largely absent.

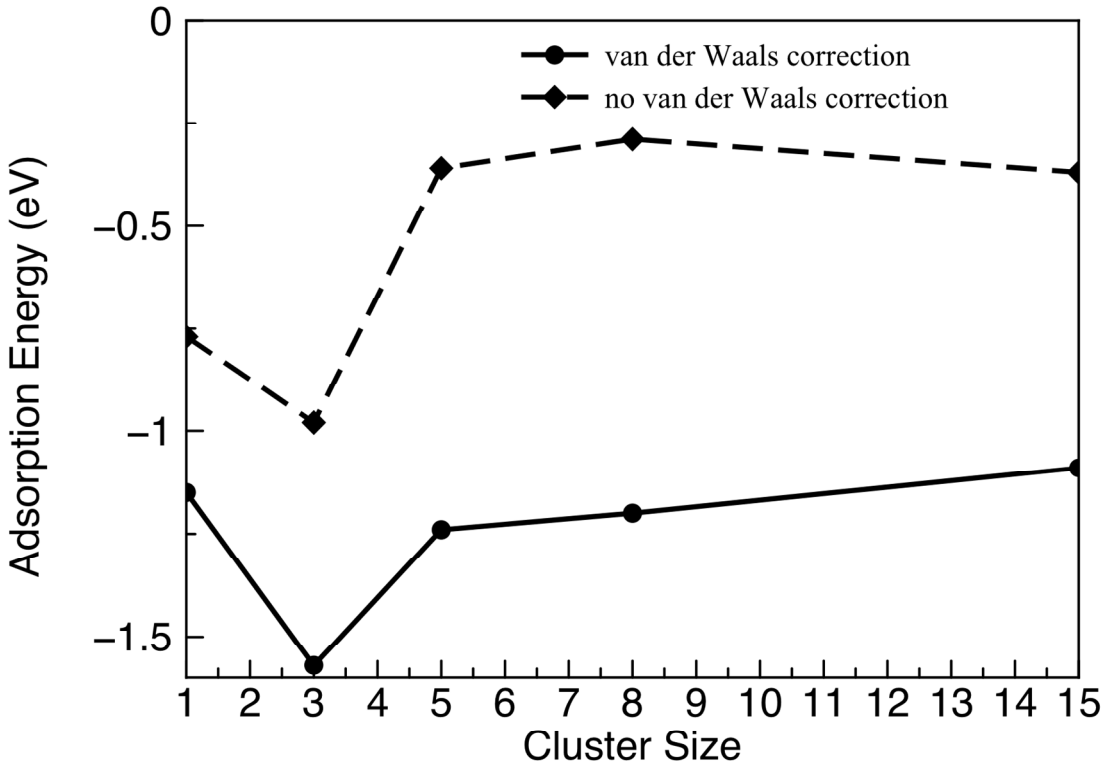

Figure 6. Comparison of TiO2 adsorption energies over pristine graphene with and without van der Waals corrections.

3.4. TiO_2 over Graphene with vacancies

Carbon vacancies in graphene are one common defect. We appropriately modeled a graphene sheet with one carbon vacancy and adsorbed TiO_2 clusters in the vicinity of this defect site. Figure 7 and Table 2 show the results of these calculations. The n = 1

Physical Chemistry Chemical Physics Accepted Manuscript

cluster had the strongest adsorption energy, being -4.60 eV. One O atom bonded to a nearby C atom, while the Ti atom filled the vacancy site between two C atoms. The closest Ti-C distance was 2.08 Å (a typical bond distance), while the closest O-C distance was 1.32 Å. The C atoms bonded to the TiO_2 cluster had significant distortions after adsorption, being pulled out of the plane of the graphene sheet. The C atom bonded to the O atom for instance rose ~1 Å above the graphene plane upon bonding with the TiO_2 cluster.

We observed similar results for the n=3 to 15 clusters upon adsorption near a C vacancy, but the distortions and adsorption energies were not considerable as those for the n=1 cluster. Adsorption energies varied between -1.50 and -2.36 eV for these clusters. Our calculated adsorption energy for the n = 3 cluster (-2.36 eV) over a C vacancy is very close to the value reported by Geng et al. (-2.43 eV)[16]. Ti-C and O-C bond distances also

Physical Chemistry Chemical Physics Accepted Manuscript

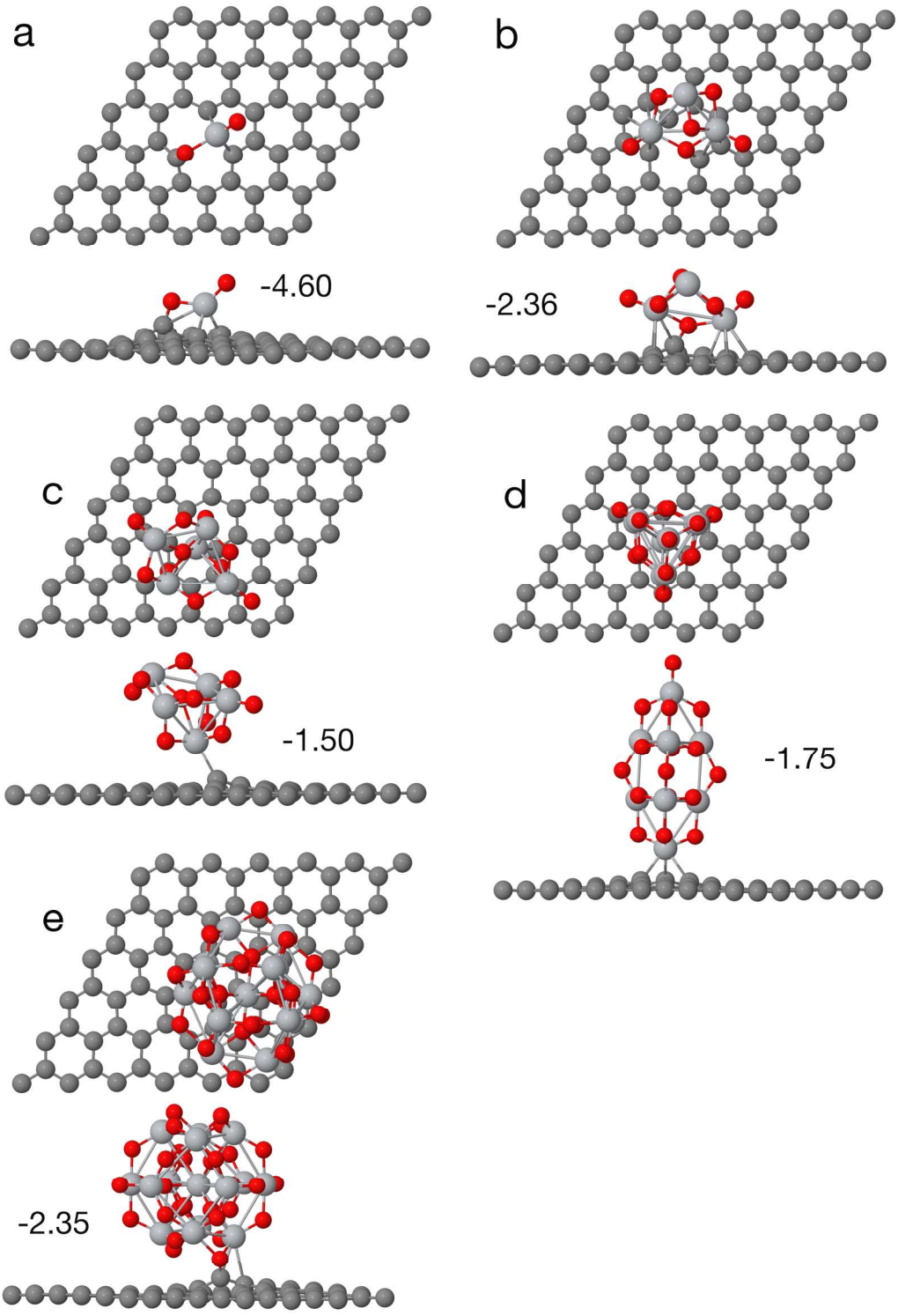

Figure 7. Most stable adsorption sites of TiO_2 clusters over graphene with a single C vacancy. Results are for clusters of size (a) n=1, (b) n=3, (c) n=5, (d) n=8, and (e) n=15. Color scheme is same as Figures 1 and 3. The numbers indicate the adsorption energies in eV.

Physical Chemistry Chemical Physics Accepted Manuscript

varied from 2.08 to 2.42 Å, and 1.32 to 2.85 Å, respectively. The more stable adsorption energies for the clusters near C vacancies compared to the pristine graphene indicate that that covalent bonding may be taking place since the C atoms near the vacancy have unsaturated bonds. This point is further illustrated in Figure 8, which shows the density of states for several carbon atoms, including a carbon atom in pristine graphene, the two carbon atoms near a C vacancy (no cluster adsorbed), and the carbon atom that is bonded to the $(TiO_2)_{15}$ cluster over a surface with carbon vacancy (see Figure 7). This latter atom bonds to the cluster and is raised significantly above the surface. The density of states illustrates that carbon atoms near a vacancy have very different electronic structure than carbon atoms in pristine graphene, which is understandable since the carbon vacancy creates a deficiency in bonds to these atoms. However, upon TiO_2 adsorption, the carbon atom that bonds to the cluster develops an electronic structure very similar to carbon atoms in pure graphene (see top and bottom plots in Figure 8). The bonding of this carbon atom to the TiO_2 cluster allows the carbon atom to achieve three stable bonds with neighboring atoms, essentially leading to a stable configuration. Furthermore, we analyzed the ratio of the number of s electrons to p electrons in these carbon atoms. Carbon atoms in pure graphene have sp^2 hybridization and integrating the density of states indicates a calculated s:p ratio of 2.06, very close to the optimal value of 2. However for the carbon atoms near the vacancy, values of 1.87 and 1.84 were calculated. In contrast, the carbon atom near the vacancy that is bonded to the TiO_2 cluster has a calculated s:p ratio of 2.02, very similar to the ratio in pure graphene which is fully bonded.

Physical Chemistry Chemical Physics Accepted Manuscript

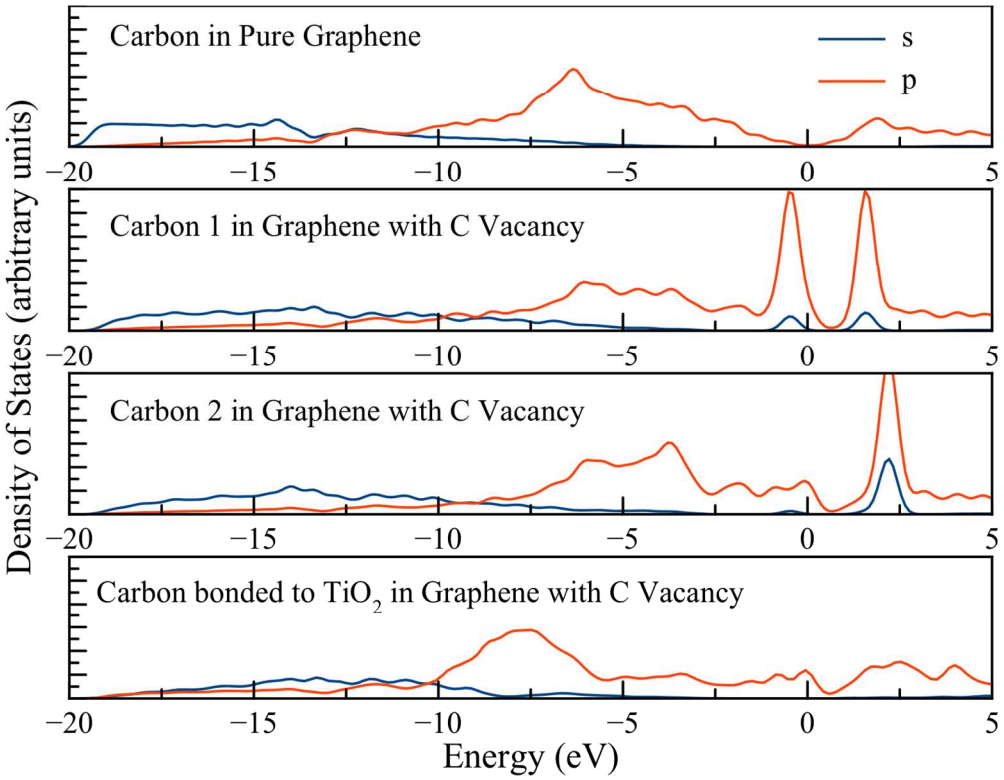

Figure 8. Density of states for various C atoms, including pure graphene, two carbon atoms near a C vacancy, and the C atom bonded to the n = 15 cluster in a surface with C vacancy.

We note that similar results of strong binding in C vacancies have been observed for metal clusters binding to graphene, where it has been shown that C vacancies can serve as anchoring sites for metals with significant distortion around the vacancy site[78, 79]. In contrast, adsorption energies for metal clusters can be much higher in magnitude than the metal oxide clusters. For example the adsorption energy was calculated to be -7.45 eV for a Pt cluster over a C vacancy in graphene[80]. While strong bonding can occur between metal oxide cluster and graphene surface, the ionic nature of the metal oxide clusters leads to relatively weaker bonding compared to the covalent bonding between metal cluster and graphene.

Physical Chemistry Chemical Physics Accepted Manuscript

3.5. TiO_2 over graphene with epoxides

Introduction of epoxide defects leads to the possibility of strong interactions between O atoms from the graphene surface with Ti atoms in the TiO_2 clusters. Our results show adsorption energies between -2.47 and -2.93 eV (Table 2), which are generally larger in magnitude than over pristine graphene or graphene with C vacancy. Indeed, for all the most stable clusters, the O atoms of graphene and Ti atoms of the clusters formed bonds that strongly anchored the clusters to graphene. The Ti-C bond distances ranged between 3.04 and 3.18 Å, which are much larger than previous results reported herein. The Ti-$O_{epoxide}$ distances however were between 1.86 and 2.00 Å, a distance equivalent to Ti-O bond lengths in TiO_2 systems.

Figure 9 shows that the epoxide O atoms serve as anchor sites for the TiO_2 clusters. The surface Ti atoms of the clusters are under-coordinated and prefer to bond to O atoms, hence the strong bonding to the epoxide O atoms. Similar behavior was seen in previous DFT studies. Ayissi et al.[18] observed stronger bonding for the n = 1 cluster over an edge epoxide site compared to pristine graphene by ~0.6 eV, while Geng et al.[16] calculated the binding energy to stabilize by ~2.1 eV for the n = 3 cluster over an epoxide compared to pristine graphene. A number of papers have indicated that reduced graphene oxide, a common form of graphene, may have oxygen-containing surface groups, particularly epoxide groups, even after synthesis[38, 40, 81, 82]. Graphene oxide is another promising photocatalytic material that has an abundant number of epoxide groups and may be interfaced with TiO_2[83-85]. Our results thus indicate that TiO_2 (or other metal oxides) are likely to bind to graphene surface through epoxide groups that may be present

Physical Chemistry Chemical Physics Accepted Manuscript

due to the synthesis approach or material. Since TiO_2 is so mobile over pristine graphene (see Figure 5), a TiO_2 particle may traverse the graphene surface until it encounters a defect, such as epoxide or vacancy, and will become immobile through strong binding to that site. This would indicate that defects and epoxide groups may play an important role in TiO_2/graphene heterostructures.

Physical Chemistry Chemical Physics Accepted Manuscript

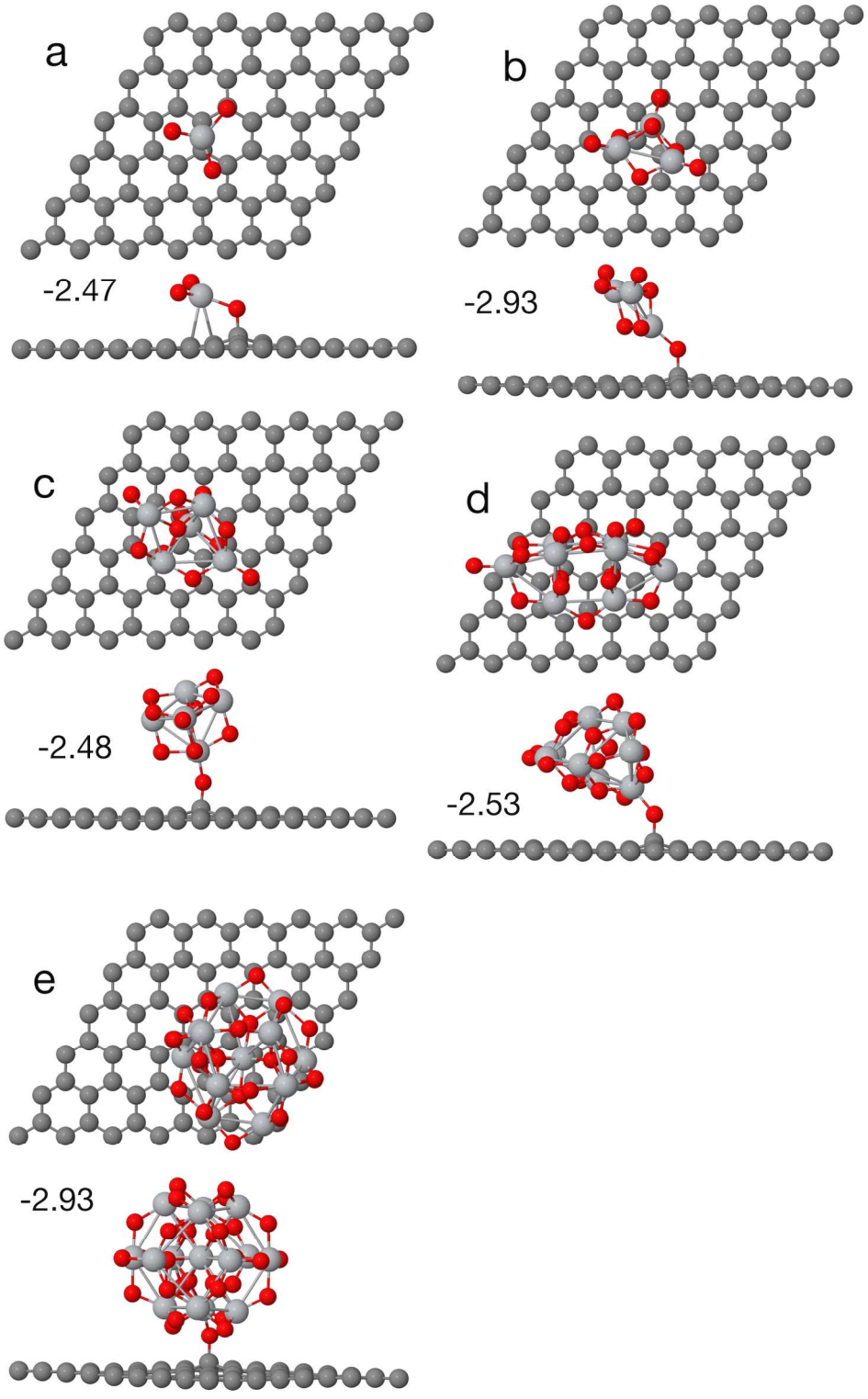

Figure 9. Most stable adsorption sites of TiO_2 clusters over graphene with a single epoxide. Results are for clusters of size (a) n=1, (b) n=3, (c) n=5, (d) n=8, and (e) n=15. Color scheme is same as Figures 1 and 3. The numbers indicate the adsorption energies in eV.

Physical Chemistry Chemical Physics Accepted Manuscript

3.6. TiO_2 over Graphene with hydroxyls

The last case we considered was adsorption of TiO_2 clusters over graphene with surface hydroxyls. Different than previous graphene surfaces studied so far, adsorption of TiO_2 clusters led to formation of oxidized $(TiO_2)_nOH$ clusters. The calculated adsorption energies varied between -2.40 and -3.59 eV, similar in magnitude to the epoxide case (see Figure 10). The hydroxyls, however, do not stay bound to the graphene upon transfer to TiO_2. The epoxide O atoms bridged the TiO_2 clusters and graphene (anchoring the TiO_2 to the surface), but no such behavior is observed for the OH groups. The OH groups clearly are part of the TiO_2 cluster rather than part of the graphene surface. Indeed, many of the newly formed clusters appear detached from the graphene surface, which we further examine.

We examined the reaction of the OH group with the TiO_2 clusters in further detail by considering two different processes, those indicated in Equations 2 and 3.

$$(TiO_2)_n + OH_{graph} \rightarrow (TiO_2)_nOH_{ads} \quad (2)$$

$$(TiO_2)_nOH_{ads} \rightarrow (TiO_2)_nOH_{gas} \quad (3)$$

Equation 2 represents the energy released upon adsorption/reaction and these energies are shown in Figure 10. Once a $(TiO_2)_nOH$ cluster forms it may desorb into gas phase (Equation 3). If the interactions between the hydroxylated cluster and graphene are favorable, then the process in Equation 3 will be endothermic, whereas if these interactions are negligible the process will be exothermic or of low magnitude. We calculated the desorption energies for the $(TiO_2)_nOH$ clusters by moving these clusters away from the surface (8 to 10 Å away), and the calculated desorption energies for the different clusters were calculated to be 0.84, 1.30, 1.19, 1.41 and 1.34 eV for the n = 1, 3,

Physical Chemistry Chemical Physics Accepted Manuscript

5, 8, and 15 clusters, respectively. The negative of these energies are essentially the adsorption energies for $(TiO_2)_nOH$ clusters over pristine graphene; such energies are comparable in size to the adsorption energies of $(TiO_2)_n$ clusters over pristine graphene. This would indicate that van der Waals forces are the main binding force between graphene and the $(TiO_2)_nOH$ clusters. Distances between the graphene surface and $(TiO_2)_nOH$ clusters (defined as closest atom in cluster to C atom of graphene) varied between 1.50 and 2.77 Å, of similar magnitude as the distances for $(TiO_2)_n$ clusters over pristine graphene. Our analysis thus indicates that hydroxylated clusters interact similarly to graphene as non-hydroxylated clusters over graphene, and that the energies released when TiO_2 clusters interact with hydroxylated graphene may be considered a sum of (a) reaction between OH and TiO_2 cluster where OH binds to uncoordinated Ti sites, and (b) van der Waals interactions that keep the cluster bound to the graphene surface.

Physical Chemistry Chemical Physics Accepted Manuscript

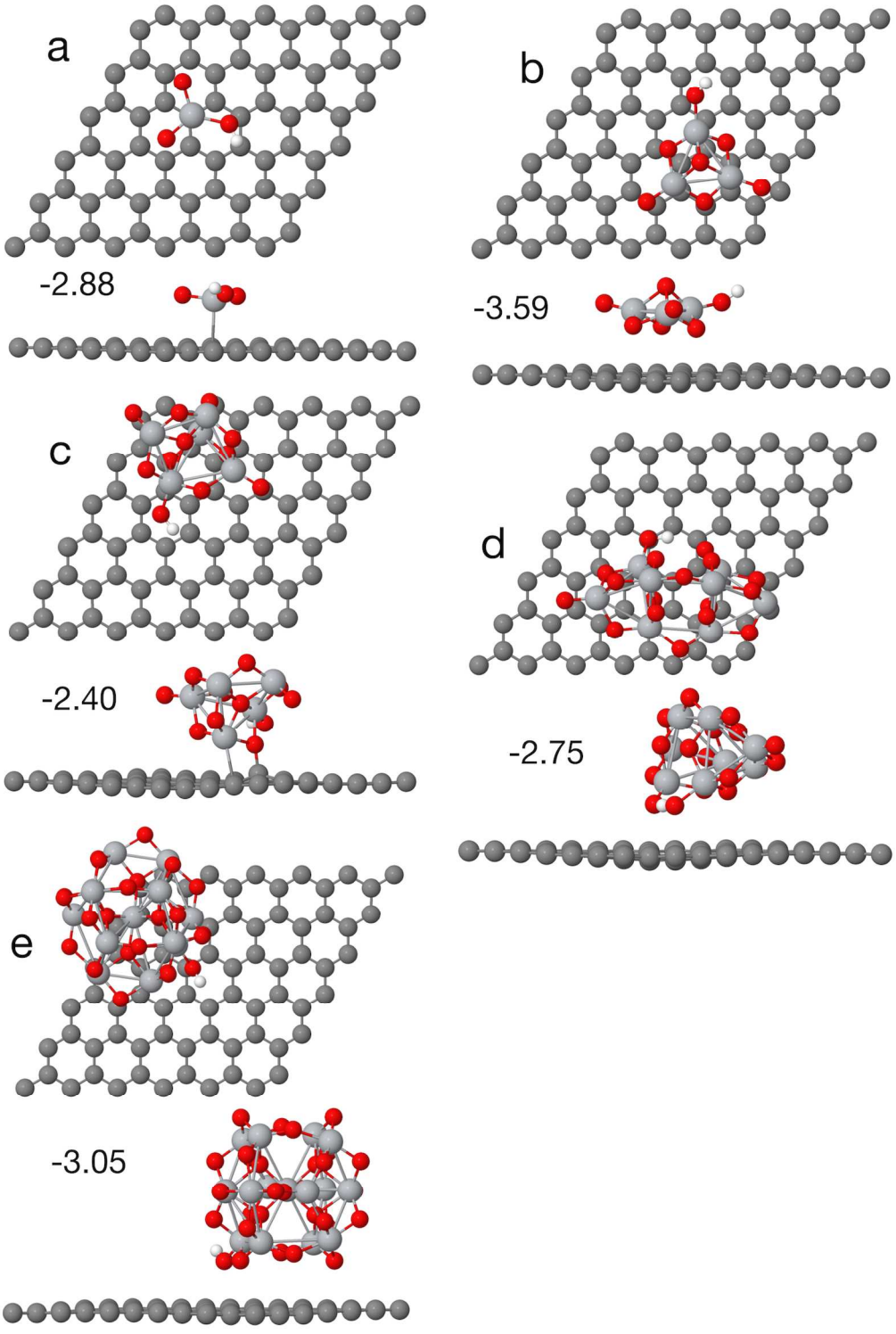

Figure 10. Most stable adsorption sites of TiO_2 clusters over graphene with a single hydroxyl. Results are for clusters of size (a) n=1, (b) n=3, (c) n=5, (d) n=8, and (e) n=15. Color scheme is same as Figures 1 and 3. The numbers indicate the adsorption energies in eV.

Physical Chemistry Chemical Physics Accepted Manuscript

3.7. Electronic Nature of TiO_2/Graphene

Beyond analyzing the binding structures of the TiO_2 clusters to graphene surfaces we also analyzed the electronic structure of these systems in order to better understand their photocatalytic properties and the nature of such composite systems. As mentioned in the methodology, these results were obtained using the VASP program with a high number of k-points (4x4x1 k-point mesh) to ensure accuracy. We first calculated Bader charges[86, 87] for the clusters over the various surfaces. For the case of the surfaces with epoxide and hydroxyls we included the O/OH groups in the analysis since the geometries denote that these groups became part of the TiO_2 clusters upon adsorption. Table 2 shows these results and indicates that electron transfer is occurring from graphene to the TiO_2 clusters as all clusters were negatively charged. This charge transfer from graphene surfaces to TiO_2 has previously been observed and rationalized based on the work functions of the two components[13]. Little charge transfer occurs over the pristine graphene surfaces and slightly more charge transfer occurs over the surfaces with C vacancies. The clusters with epoxide or hydroxyl have significantly more negative charge, largely due to the presence of the extra O/OH. O atoms in TiO_2 have nominal charges of -2 so inclusion of an extra O atom in the TiO_2 clusters understandably lowers the charge. In the case of the clusters with hydroxyl the clusters have significant negative charge. The presence of hydrogen atom (which has nominal charge of +1) however leads to less negative charge compared to the epoxide clusters. Overall, the calculated charges indicate electron transfer occurs from graphene to TiO_2 cluster and that the amount of charge can roughly be correlated with binding energy (pristine < C vacancy < epoxide ≈ hydroxyl).

Physical Chemistry Chemical Physics Accepted Manuscript

Table 3. Calculated Bader charges for the TiO_2 clusters over the various graphene surfaces. The case of graphene with epoxide includes the epoxide O atom in the calculated charge. The case of graphene with hydroxyl includes the OH atoms in the calculated charge.

	Surface Type			
Cluster Size (n)	**Pristine graphene**	**Graphene with C vacancy**	**Graphene with epoxide**	**Graphene with hydroxyl**
1	-0.03	-0.11	-0.90	-0.43
3	-0.14	-0.02	-1.17	-0.83
5	-0.08	-0.23	-1.32	-0.63
8	-0.07	-0.15	-1.29	-0.86
15	-0.27	-0.56	-1.29	-0.80

We also performed charge density difference analysis of the n = 15 clusters to further identify the nature of the bonding between graphene and TiO_2 clusters. These results are shown in Figure 11. The charge density difference is calculated by taking the electron density of the combined graphene/TiO_2 system and subtracting the densities of the lone TiO_2 and graphene parts, albeit in the same geometry as the combined system. Such calculations indicate how electrons shift (either adding or subtracting) in certain regions of the system, and thus are indicative of bonding patterns. In the case of the graphene with hydroxyl we considered the OH to be part of TiO_2 since it has clearly migrated to the cluster, and so the graphene system in this case only contains carbon atoms. Our results show that very little electron density changes upon adsorption over pristine TiO_2, suggesting that no true chemical bonding is taking place, in agreement with our previous results. However, over graphene with a defect and graphene with epoxide there is significant electron density shift. For both these cases in the region of the C vacancy or bridging epoxide (lower left region of TiO_2 particle) the electron density is strongly changed, indicating that strong bonding occurs in this region, since the C

Physical Chemistry Chemical Physics Accepted Manuscript

vacancy or O atom bind the TiO_2 particle to the surface. For the hydroxylated TiO_2 cluster very little electron density change is observed, and the hydroxylated particle essentially interacts weakly with the graphene surface.

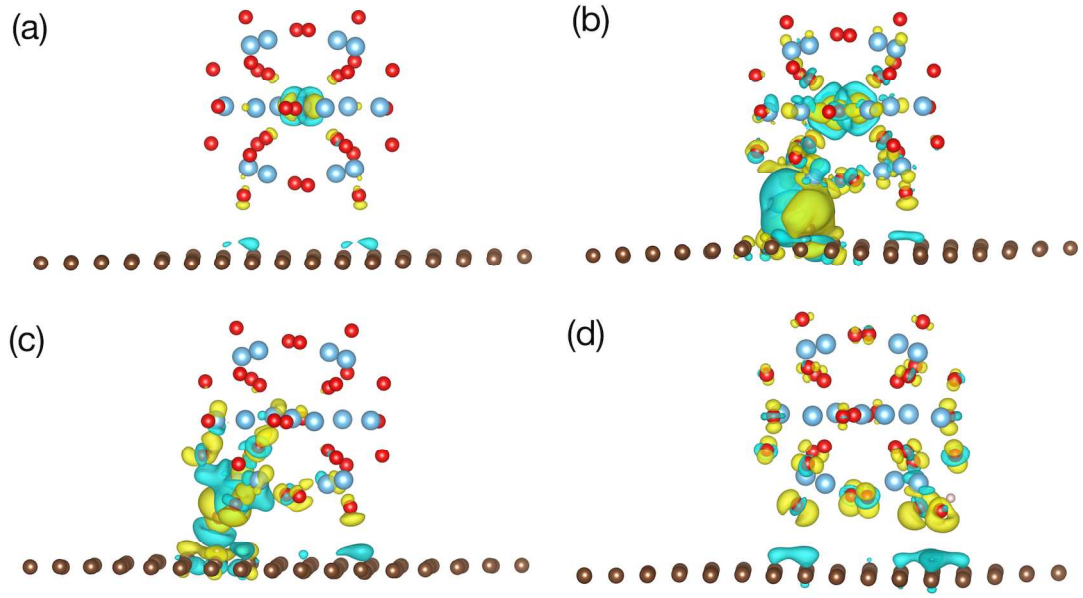

Figure 11. Charge density different plots for the $(TiO_2)_{15}$ clusters over (a) pristine graphene, (b) graphene with C vacancy, (c) graphene with epoxide, and (d) graphene with hydroxyl. Shown are contours for $4.2*10^{-7}$ $e^-/Å^3$. Blue contours correspond to negative electron density difference while yellow contours correspond to positive electron density difference. The figure was made with the VESTA 3 program[88].

We also calculated density of states (DOS) for the various graphene-TiO_2 systems. We present in Figure 12 the case for n = 15. The n = 15 cluster is representative of a larger, typical particle that may occur in graphene/TiO_2 systems[12] and is the focus of our following analysis. In the plots the graphene DOS only contain the carbon atoms, while the TiO_2 DOS includes any surface groups (epoxide/hydroxyl). A number of features are observed in the DOS plots. Since the number of electrons in the TiO_2 cluster is much larger than in the graphene surface, the TiO_2 DOS dominates the plots. The

Physical Chemistry Chemical Physics Accepted Manuscript

graphene DOS remain relatively the same throughout the different systems, with slight changes in the peak/edge positions due to changes in the Fermi level upon formation of the heterostructures. The TiO_2 DOS appear to have modest changes. For instance, in gas phase, the unoccupied DOS for TiO_2 show two peaks (top panel), whereas upon adsorption these peaks appear to merge together for several of the systems. The general structure however of the TiO_2 DOS remain unchanged, except for changes in peak positions, shifting of the valence/conduction bands, and introduction of gap states.

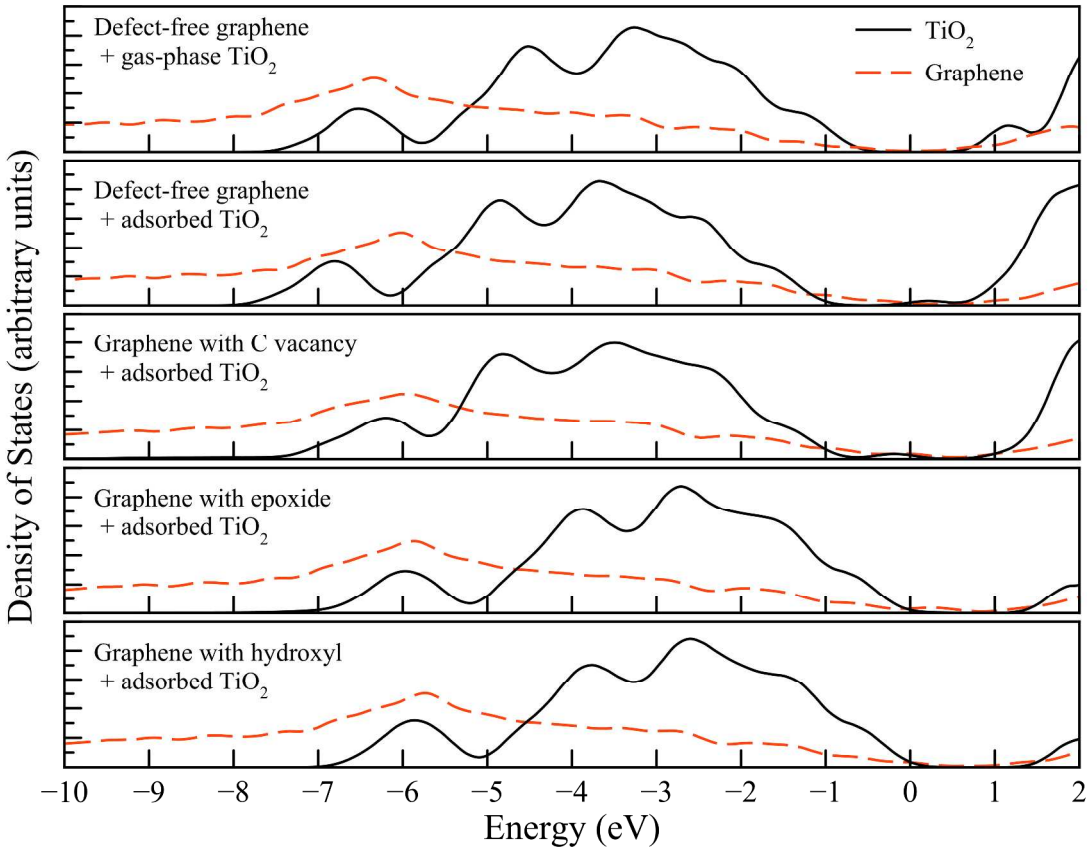

Figure 12. Density of states for the $(TiO_2)_{15}$ cluster in gas phase (top plot) and adsorbed over various graphene surfaces (as indicated in the figure). Also shown is the graphene density of states for the various systems. Zero eV corresponds to the Fermi level of each system.

Physical Chemistry Chemical Physics Accepted Manuscript

There are changes in the band gap regions of the TiO_2 clusters. For adsorption of TiO_2 over pristine graphene and over the surface with C vacancy gap states arise that may affect photoabsorption. These gap states may potentially lower the band gap by changing the highest occupied molecular orbital (HOMO) or lowest unoccupied molecular orbital (LUMO). Similar behavior was observed for crystalline TiO_2 interfaced with disordered TiO_2[89]. The latter disordered phased introduced gap states which served as LUMO states. Gap states however may also negatively impact charge recombination by acting as charge trapping sites; the more localized the gap state the more likely it is to trap charge and act as a recombination center. The observed gap states over TiO_2/graphene systems appear delocalized, so it is unclear as to how much they would affect recombination. Moreover, the difficulty in determining band gaps from DOS plots is deciding the exact location of HOMO/LUMO. These edges are sensitive for instance to choice of smearing parameters/method used to obtain the DOS. Nonetheless, we chose these edges for DOS lower than a value of 1.5 electrons/eV (in comparison highest peaks were near 50 electrons/eV). We have summarized the band gap changes for the TiO_2 clusters upon adsorption in Table 3 which shows that small changes are observed for the band gaps, with the largest change occurring for the cluster adsorbed over a C vacancy. The band gap for the TiO_2 cluster decreases by 0.31 eV in this case. Interestingly, the band gaps for all TiO_2 clusters slightly increase for the epoxide/hydroxyl surfaces. A small decrease (0.14 eV) in the band gap of TiO_2 occurs over the pristine surface. Previous DFT papers[16, 18] observed little change in the band gap for TiO_2 upon contact with graphene, in agreement with our work.

Physical Chemistry Chemical Physics Accepted Manuscript

Table 3. Calculated changes in band gap of the $(TiO_2)_{15}$ cluster upon adsorption over various graphene surfaces relative to the gas-phase cluster. Positive numbers indicate increased band gap relative to gas-phase, while negative numbers indicated decreased band gap relative to gas-phase.

Graphene Surface	$\Delta E_{band\ gap}$ (eV)
Pristine graphene	-0.14
Graphene with C vacancy	-0.31
Graphene with epoxide	0.11
Graphene with hydroxyl	0.13

3.8. Implications on the Photocatalytic Behavior of TiO_2/Graphene

Several explanations exist as to why TiO_2/graphene composites are so photocatalytically active. Experimental results[90] suggest that due to the high charge mobility of graphene, charge can be transferred to graphene and increase their mobility/lifetime. Visible light photoexcitation is observed in TiO_2/graphene materials[11-13], which increases photoexcitation efficiency. Other results suggest that TiO_2 may be photosensitized in the presence of graphene oxide, decreasing the observed band gap[42]. A still, largely unexplored potential reason is that new active reaction sites may be created at/near the interface.

A variety of previously reported DFT results are available in the literature on the electronic transitions between graphene and TiO_2. Calculations[13, 24] indicate that a rutile slab in contact with graphene could lead to greater photoexcitation yield as valence electrons in graphene may be excited to conduction levels in TiO_2, requiring less energy for photoexcitation than the pure band gap of rutile. In contrast other DFT calculations[25] showed the opposite for an anatase slab over graphene; TiO_2 valence electrons may be photoexcited to graphene conduction bands. Still another set of calculations[27, 32] for anatase over graphene predicted that electrons predominantly localized in graphene can

Physical Chemistry Chemical Physics Accepted Manuscript

be photoexcited to states predominantly localized in TiO_2. Other work[26] on anatase over graphene observed broad gap states that may improve photoexcitation. This quick overview of DFT studies illustrates the difficulty with TiO_2/graphene materials, since many different (sometimes contrary) results can be obtained. Likely the choice of system size and simulation parameters all contribute to different results. For instance, several studies used the local density approximation (LDA) exchange correlation functional, which is generally not as accurate as generalized gradient approximation (GGA) functionals. Small simulation cells used in some studies may be more computationally tractable, but introduce unrealistic strain. The advantage of the current results are that we utilize the GGA exchange correlation functional in combination with a van der Waals correction and the +U correction, as well as a large simulation cell, to give accurate energies/electronic structure with no strain-related errors.

As indicated in the previous section, modest changes are observed in the band gap of TiO_2 upon graphene adsorption and we therefore do not expect TiO_2 valence to conduction band electronic excitation to explain the improved capability of TiO_2/graphene materials. Synergy between TiO_2 and graphene however can lead to new photoexcitation properties. Figure 13 shows a close-up of the gap region of for the n = 15 clusters adsorbed over various surfaces. For TiO_2 adsorbed over pure graphene we observe that excitation from graphene to TiO_2 is possible, since the bands below the Fermi level are predominantly on graphene, while bands above the Fermi level are centered on TiO_2 (in agreement with previous results[13, 24]). For TiO_2 over a C vacancy there is much more overlap between the various bands; near the Fermi level it is hard to distinguish the dominating bands since the two materials have such similar bands. This

Physical Chemistry Chemical Physics Accepted Manuscript

suggests that it is hard to distinguish whether excitation may occur from either graphene/TiO_2 to graphene/TiO_2. For TiO_2 over the surface with epoxide photoexcitation may occur from TiO_2 to graphene. Finally for TiO_2 over the surface with hydroxyl photoexcitation may occur from TiO_2 to graphene. Our results show a variety of possible photoexcitation events, with the surface structure determining what direction electrons may flow. We acknowledge that our analysis of charge transfer between TiO_2 and graphene is based on overlap of the density of states, and that the transition probability between the two materials must be taken into account. Other time-dependent DFT results[24], however showed that rapid electron transfer occurs between TiO_2 and graphene, suggesting a high transition probability between the two materials. Our results nonetheless will certainly have important implications on TiO_2/graphene catalysts since charge separation is a key phenomena associated with these materials. For instance, TiO_2 bound by epoxide may have electrons transferred to graphene, leading to increased charge separation since graphene has high electrical conductivity and such electrons may move away from TiO_2.

Physical Chemistry Chemical Physics Accepted Manuscript

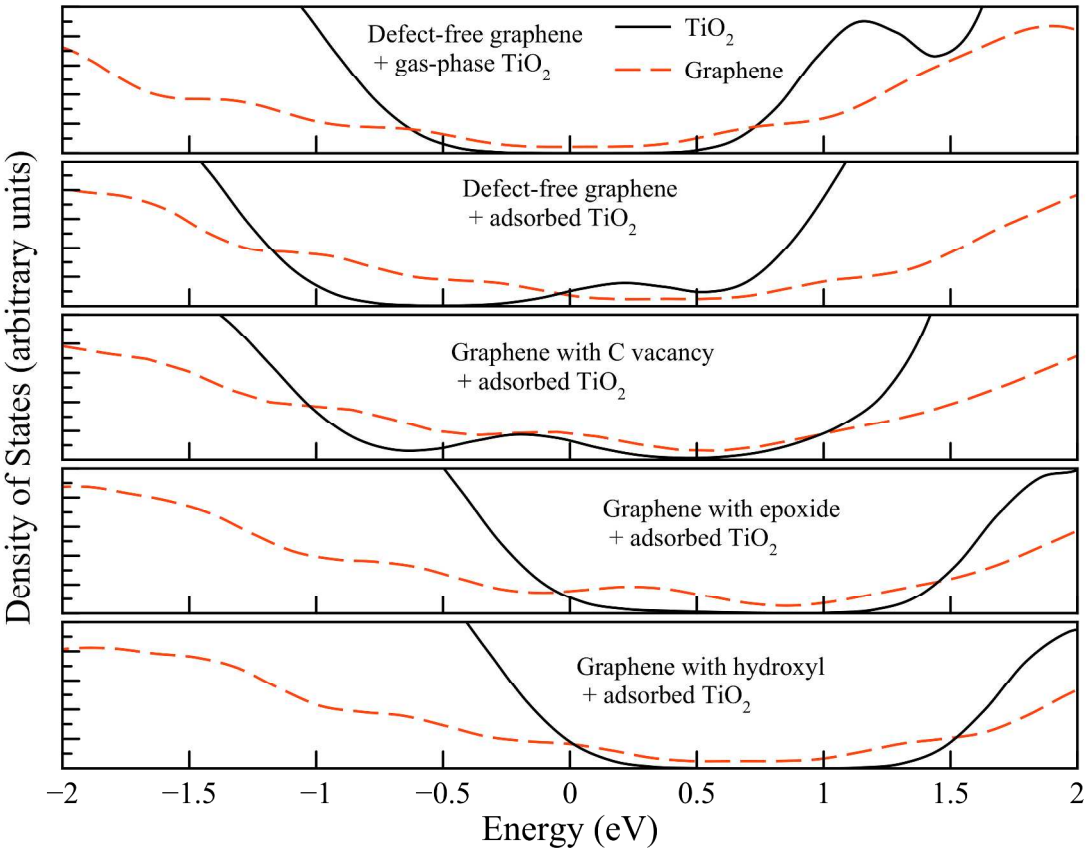

Figure 13. Density of states for the $(TiO_2)_{15}$ cluster in gas phase (top plot) and adsorbed over various graphene surfaces (as indicated in the figure) in the region of the band gap. Also shown is the graphene density of states for the various systems. Zero eV corresponds to the Fermi level of each system. Note that the x and y axis scales are not the same as those in Figure 12 since the current figure shows the close-up details of the gap region.

Various publications have indicated that intimate contact between TiO_2 and graphene gives better photocatalytic activity[12, 91, 92]. Indeed, functionalization of graphene through various surface groups is one approach to better TiO_2/graphene materials since such surface groups may be nucleation sites for TiO_2[93]. This concept is consistent with our current work, which demonstrates that oxygen-containing groups or defects significantly enhance interactions between graphene and TiO_2 and strongly bind nanoparticles. Still, more work is needed to understand these composite materials. Experimental work[91, 94], for instance, suggests that defects (such as those present in

Physical Chemistry Chemical Physics Accepted Manuscript

reduced graphene oxide) may impede TiO_2/graphene activity since this lowers the electrical conductivity of graphene. These defects may be undesirable for purposes of charge transport in graphene (lowered charge transport or increased charge trapping) and therefore affect charge recombination/mobility negatively. However increased defects and surface groups may lead to greater photocatalyst stability as well as more charge transfer between graphene and TiO_2. More work is needed to understand the counter-play between these two effects and the ideal state for fast charge mobility in graphene and good contact/stability between TiO_2 and graphene.

4.0. Conclusions

In this work we simulated the adsorption of TiO_2 clusters onto several graphene surfaces, including pristine surfaces and surfaces with C vacancies, epoxide groups, and hydroxyl groups. "Real" graphene surfaces often have various defects or surface groups, depending on synthesis procedure. Adsorption over pristine graphene surfaces had the weakest adsorption energies and was driven by van der Waals interactions between TiO_2 and graphene. However, adsorption of TiO_2 over graphene with C vacancies or epoxide groups leads to strong binding. When TiO_2 interacts with a surface hydroxyl, full transfer of the hydroxyl to the TiO_2 cluster is observed and the process is highly exothermic. These results suggest that different surface inhomogeneities on graphene may serve to anchor TiO_2 to its surface, while TiO_2 over pure graphene may more freely move or slide across the surface. Analysis of the electronic properties of these composites indicates that photoexcitation between TiO_2 and graphene can occur in various ways, depending on the graphene surface structure. Over pure graphene, for instance, graphene to TiO_2 electronic

Physical Chemistry Chemical Physics Accepted Manuscript

excitation can occur, while over surfaces with epoxides or hydroxyls TiO_2 to graphene electronic excitation can occur. Our work highlights the important role of graphene surface structure in these composites.

Acknowledgments

We wish to thank Sia Najafi of WPI for his help in using the WPI computers. We also thank the Environmental Molecular Science Laboratory (EMSL) at Pacific Northwest National Laboratory in Richland, WA for providing computational resources. EMSL is a DOE Office of Science User Facility sponsored by the Office of Biological and Environmental Research and located at Pacific Northwest National Laboratory.

References

1. X. Q. An and J. C. Yu, *RSC Advances*, 2011, **1**, 1426-1434.
2. D. A. C. Brownson, D. K. Kampouris and C. E. Banks, *Chemical Society Reviews*, 2012, **41**, 6944-6976.
3. H. Chang and H. Wu, *Energy & Environmental Science*, 2013, **6**, 3483-3507.
4. D. Chen, H. Zhang, Y. Liu and J. Li, *Energy & Environmental Science*, 2013, **6**, 1362-1387.
5. C. Huang, C. Li and G. Shi, *Energy & Environmental Science*, 2012, **5**, 8848-8868.
6. H. Y. Mao, S. Laurent, W. Chen, O. Akhavan, M. Imani, A. A. Ashkarran and M. Mahmoudi, *Chemical Reviews*, 2013, **113**, 3407-3424.
7. Y. B. Tan and J.-M. Lee, *Journal of Materials Chemistry A*, 2013, **1**, 14814-14843.
8. N. Mahmood, C. Zhang, H. Yin and Y. Hou, *Journal of Materials Chemistry A*, 2014, **2**, 15-32.
9. S. Morales-Torres, L. Pastrana-Martínez, J. Figueiredo, J. Faria and A. T. Silva, *Environ Sci Pollut Res*, 2012, **19**, 3676-3687.
10. P. T. Yin, T.-H. Kim, J.-W. Choi and K.-B. Lee, *Physical Chemistry Chemical Physics*, 2013, **15**, 12785-12799.

Physical Chemistry Chemical Physics Accepted Manuscript

11. H. Zhang, X. J. Lv, Y. M. Li, Y. Wang and J. H. Li, *Acs Nano*, 2010, **4**, 380-386.
12. M. Long, Y. Qin, C. Chen, X. Guo, B. Tan and W. Cai, *The Journal of Physical Chemistry C*, 2013, **117**, 16734-16741.
13. A. Du, Y. H. Ng, N. J. Bell, Z. Zhu, R. Amal and S. C. Smith, *The Journal of Physical Chemistry Letters*, 2011, **2**, 894-899.
14. R. K. Upadhyay, N. Soin and S. S. Roy, *RSC Advances*, 2014, **4**, 3823-3851.
15. R. Leary and A. Westwood, *Carbon*, 2011, **49**, 741-772.
16. W. Geng, H. Liu and X. Yao, *Physical Chemistry Chemical Physics*, 2013, **15**, 6025-6033.
17. M. Favaro, S. Agnoli, C. Di Valentin, C. Mattevi, M. Cattelan, L. Artiglia, E. Magnano, F. Bondino, S. Nappini and G. Granozzi, *Carbon*, 2014, **68**, 319-329.
18. S. Ayissi, P. A. Charpentier, N. Farhangi, J. A. Wood, K. Palotás and W. A. Hofer, *The Journal of Physical Chemistry C*, 2013, **117**, 25424-25432.
19. M. I. Rojas and E. P. M. Leiva, *Physical Review B*, 2007, **76**, 155415.
20. E. H. Song and Y. F. Zhu, *Nanoscience and Nanotechnology Letters*, 2013, **5**, 198-203.
21. L. Wang, J. Zhao, L. Wang, T. Yan, Y.-Y. Sun and S. B. Zhang, *Physical Chemistry Chemical Physics*, 2011, **13**, 21126-21131.
22. Y. Yuan, X. Gong and H. Wang, *Physical Chemistry Chemical Physics*, 2015, **17**, 11375-11381.
23. N. Farhangi, S. Ayissi and P. A. Charpentier, *Nanotechnology*, 2014, **25**, 305601.
24. R. Long, N. J. English and O. V. Prezhdo, *Journal of the American Chemical Society*, 2012, **134**, 14238-14248.
25. H. Gao, X. Li, J. Lv and G. Liu, *The Journal of Physical Chemistry C*, 2013, **117**, 16022-16027.
26. N. Yang, Y. Liu, H. Wen, Z. Tang, H. Zhao, Y. Li and D. Wang, *ACS Nano*, 2013, **7**, 1504-1512.
27. X. Li, H. Gao and G. Liu, *Journal*, 2013, **1025**, 30-34.
28. J. Tang, Y. Zhang, B. Kong, Y. Wang, P. Da, J. Li, A. A. Elzatahry, D. Zhao, X. Gong and G. Zheng, *Nano Letters*, 2014, **14**, 2702-2708.
29. G. Mogilevsky, O. Hartman, E. D. Emmons, A. Balboa, J. B. DeCoste, B. J. Schindler, I. Iordanov and C. J. Karwacki, *ACS Applied Materials & Interfaces*, 2014, **6**, 10638-10648.
30. S. Umrao, S. Abraham, F. Theil, S. Pandey, V. Ciobota, P. K. Shukla, C. J. Rupp, S. Chakraborty, R. Ahuja, J. Popp, B. Dietzek and A. Srivastava, *RSC Advances*, 2014, **4**, 59890-59901.
31. M.-h. Wang, Y.-n. Guo, Q. Wang, X.-s.-y. Zhang, J.-j. Huang, X. Lu, K.-f. Wang, H.-p. Zhang and Y. Leng, *Chemical Physics Letters*, 2014, **599**, 86-91.
32. Y. Masuda, G. Giorgi and K. Yamashita, *physica status solidi (b)*, 2014, **251**, 1471-1479.
33. W. Choi, I. Lahiri, R. Seelaboyina and Y. S. Kang, *Critical Reviews in Solid State and Materials Sciences*, 2010, **35**, 52-71.
34. Y. Zhu, S. Murali, W. Cai, X. Li, J. W. Suk, J. R. Potts and R. S. Ruoff, *Advanced Materials*, 2010, **22**, 3906-3924.
35. M. J. Allen, V. C. Tung and R. B. Kaner, *Chemical Reviews*, 2009, **110**, 132-145.

Physical Chemistry Chemical Physics Accepted Manuscript

36. F. Banhart, J. Kotakoski and A. V. Krasheninnikov, *ACS Nano*, 2010, **5**, 26-41.
37. J. Ito, J. Nakamura and A. Natori, *Journal of Applied Physics*, 2008, **103**, -.
38. S. Stankovich, D. A. Dikin, R. D. Piner, K. A. Kohlhaas, A. Kleinhammes, Y. Jia, Y. Wu, S. T. Nguyen and R. S. Ruoff, *Carbon*, 2007, **45**, 1558-1565.
39. C. Mattevi, G. Eda, S. Agnoli, S. Miller, K. A. Mkhoyan, O. Celik, D. Mastrogiovanni, G. Granozzi, E. Garfunkel and M. Chhowalla, *Advanced Functional Materials*, 2009, **19**, 2577-2583.
40. A. Bagri, C. Mattevi, M. Acik, Y. J. Chabal, M. Chhowalla and V. B. Shenoy, *Nat Chem*, 2010, **2**, 581-587.
41. T.-F. Yeh, J. Cihlář, C.-Y. Chang, C. Cheng and H. Teng, *Materials Today*, 2013, **16**, 78-84.
42. C. Chen, W. Cai, M. Long, B. Zhou, Y. Wu, D. Wu and Y. Feng, *ACS Nano*, 2010, **4**, 6425-6432.
43. G. Lippert, J. Hutter and M. Parrinello, *Theoretical Chemistry Accounts*, 1999, **103**, 124-140.
44. J. VandeVondele and J. Hutter, *J. Chem. Phys.*, 2007, **127**.
45. S. Goedecker, M. Teter and J. Hutter, *Physical Review B*, 1996, **54**, 1703-1710.
46. M. Krack, *Theoretical Chemistry Accounts*, 2005, **114**, 145-152.
47. J. P. Perdew, K. Burke and M. Ernzerhof, *Phys. Rev. Lett.*, 1996, **77**, 3865-3868.
48. S. Grimme, *Journal of Computational Chemistry*, 2006, **27**, 1787-1799.
49. http://www.cp2k.org, *CP2K developers home page*, 2015.
50. J. VandeVondele, M. Krack, F. Mohamed, M. Parrinello, T. Chassaing and J. Hutter, *Comput Phys Commun*, 2005, **167**, 103-128.
51. G. Kresse and J. Hafner, *Physical Review B*, 1993, **47**, 558-561.
52. G. Kresse and J. Hafner, *Physical Review B*, 1994, **49**, 14251-14269.
53. G. Kresse and J. Furthmuller, *Comput. Mater. Sci.*, 1996, **6**, 15-50.
54. G. Kresse and J. Furthmuller, *Physical Review B*, 1996, **54**, 11169-11186.
55. G. Kresse and D. Joubert, *Physical Review B*, 1999, **59**, 1758-1775.
56. P. E. Blöchl, *Physical Review B*, 1994, **50**, 17953-17979.
57. S. L. Dudarev, G. A. Botton, S. Y. Savrasov, C. J. Humphreys and A. P. Sutton, *PHYSICAL REVIEW B*, 1998, **57**, 1505-1509.
58. J. C. Garcia, M. Nolan and N. A. Deskins, *The Journal of Chemical Physics*, 2015, **142**, 024708.
59. B. J. Morgan and G. W. Watson, *Surface Science*, 2007, **601**, 5034-5041.
60. B. J. Morgan and G. W. Watson, *The Journal of Physical Chemistry C*, 2010, **114**, 2321-2328.
61. T. Shibuya, K. Yasuoka, S. Mirbt and B. Sanyal, *Journal of physics. Condensed matter : an Institute of Physics journal*, 2012, **24**, 435504-435504.
62. A. Iwaszuk, P. a. Mulheran and M. Nolan, *Journal of Materials Chemistry A*, 2013, **1**, 2515-2515.
63. A. Iwaszuk and M. Nolan, *The Journal of Physical Chemistry C*, 2011, **115**, 12995-13007.
64. A. Iwaszuk and M. Nolan, *Journal of Materials Chemistry A*, 2013, **1**, 6670-6670.
65. A. Iwaszuk and M. Nolan, *Physical chemistry chemical physics : PCCP*, 2011, **13**, 4963-4973.

Physical Chemistry Chemical Physics Accepted Manuscript

66. Z. W. Qu and G. J. Kroes, *Journal of Physical Chemistry B*, 2006, **110**, 8998-9007.
67. S. Hamad, C. R. A. Catlow, S. M. Woodley, S. Lago and J. A. Mejías, *The journal of physical chemistry. B*, 2005, **109**, 15741-15748.
68. M. n. Calatayud, L. Maldonado and C. Minot, *Journal of Physical Chemistry C*, 2008, **112**, 16087-16095.
69. M. n. Calatayud and C. Minot, *The Journal of Physical Chemistry C*, 2009, **113**, 12186-12194.
70. A. D. Becke, *The Journal of Chemical Physics*, 1993, **98**, 5648-5652.
71. P. J. Stephens, F. J. Devlin, C. F. Chabalowski and M. J. Frisch, *The Journal of Physical Chemistry*, 1994, **98**, 11623-11627.
72. D. Vanderbilt, *Journal*, 1990, **41**, 7892-7895.
73. G. Kresse and J. Hafner, *J. Phys.: Condens. Matter*, 1994, **6**, 8245-8257.
74. J. P. Perdew, J. Chevary, S. Vosko, K. A. Jackson, M. R. Pederson, D. Singh and C. Fiolhais, *Physical Review B*, 1992, **46**, 6671.
75. M. Dion, H. Rydberg, E. Schröder, D. C. Langreth and B. I. Lundqvist, *Phys. Rev. Lett.*, 2004, **92**, 246401.
76. K. Lee, É. D. Murray, L. Kong, B. I. Lundqvist and D. C. Langreth, *Physical Review B*, 2010, **82**, 081101.
77. D. W. Boukhvalov and M. I. Katsnelson, *Journal of the American Chemical Society*, 2008, **130**, 10697-10701.
78. M. M. Ugeda, D. Fernández-Torre, I. Brihuega, P. Pou, A. J. Martínez-Galera, R. Pérez and J. M. Gómez-Rodríguez, *Phys. Rev. Lett.*, 2011, **107**, 116803.
79. D.-H. Lim, A. S. Negreira and J. Wilcox, *The Journal of Physical Chemistry C*, 2011, **115**, 8961-8970.
80. D.-H. Lim and J. Wilcox, *The Journal of Physical Chemistry C*, 2011, DOI: 10.1021/jp205244m, 111102112458009-111102112458009.
81. P. V. Kumar, M. Bernardi and J. C. Grossman, *ACS Nano*, 2013, **7**, 1638-1645.
82. S. Pei and H.-M. Cheng, *Carbon*, 2012, **50**, 3210-3228.
83. V. Stengl, S. Bakardjieva, T. M. Grygar, J. Bludska and M. Kormunda, *Chemistry Central Journal*, 2013, **7**, 41.
84. K. Krishnamoorthy, R. Mohan and S.-J. Kim, *Applied Physics Letters*, 2011, **98**, 244101.
85. T. N. Lambert, C. A. Chavez, B. Hernandez-Sanchez, P. Lu, N. S. Bell, A. Ambrosini, T. Friedman, T. J. Boyle, D. R. Wheeler and D. L. Huber, *The Journal of Physical Chemistry C*, 2009, **113**, 19812-19823.
86. R. F. W. Bader, *Accounts of Chemical Research*, 1985, **18**, 9-15.
87. G. Henkelman, A. Arnaldsson and H. Jonsson, *Comput. Mater. Sci.*, 2006, **36**, 354-360.
88. K. Momma and F. Izumi, *Journal of Applied Crystallography*, 2011, **44**, 1272-1276.
89. X. Chen, L. Liu, P. Y. Yu and S. S. Mao, *Science*, 2011, **331**, 746-750.
90. N. J. Bell, Y. H. Ng, A. Du, H. Coster, S. C. Smith and R. Amal, *The Journal of Physical Chemistry C*, 2011, **115**, 6004-6009.
91. Y. Zhang, N. Zhang, Z.-R. Tang and Y.-J. Xu, *Physical Chemistry Chemical Physics*, 2012, **14**, 9167-9175.

Physical Chemistry Chemical Physics Accepted Manuscript

92. Y. Zhang, Z.-R. Tang, X. Fu and Y.-J. Xu, *ACS Nano*, 2011, **5**, 7426-7435.
93. F. Sordello, G. Zeb, K. Hu, P. Calza, C. Minero, T. Szkopek and M. Cerruti, *Nanoscale*, 2014, **6**, 6710-6719.
94. Y. T. Liang, B. K. Vijayan, K. A. Gray and M. C. Hersam, *Nano Letters*, 2011, **11**, 2865-2870.

Physical Chemistry Chemical Physics Accepted Manuscript